



HAL
open science

Kinetic Aspects of Emulsion Stabilization by Surfactants: A Microfluidic Analysis

Jean-Christophe Baret, Felix Kleinschmidt, Abdeslam El Harrak, Andrew
Griffiths

► **To cite this version:**

Jean-Christophe Baret, Felix Kleinschmidt, Abdeslam El Harrak, Andrew Griffiths. Kinetic Aspects of Emulsion Stabilization by Surfactants: A Microfluidic Analysis. *Langmuir*, 2009, 25 (11), pp.6088-6093. 10.1021/la9000472 . hal-02148749

HAL Id: hal-02148749

<https://hal.science/hal-02148749>

Submitted on 26 Mar 2021

HAL is a multi-disciplinary open access archive for the deposit and dissemination of scientific research documents, whether they are published or not. The documents may come from teaching and research institutions in France or abroad, or from public or private research centers.

L'archive ouverte pluridisciplinaire **HAL**, est destinée au dépôt et à la diffusion de documents scientifiques de niveau recherche, publiés ou non, émanant des établissements d'enseignement et de recherche français ou étrangers, des laboratoires publics ou privés.

Kinetic aspects of emulsion stabilization by surfactants : a microfluidic analysis

Jean-Christophe Baret*, Felix Kleinschmidt*,
Abdeslam El Harrak*, and Andrew D. Griffiths*

March 26, 2021

This is the author version of the manuscript published as *Kinetic aspects of emulsion stabilization by surfactants : a microfluidic analysis*, JC. Baret et al. Langmuir 2009 (DOI:10.1021/la9000472)

*Institut de Science et d'Ingénierie Supramoléculaires (ISIS), Université de Strasbourg (UdS), CNRS UMR 7006, Strasbourg (France).

Abstract

In classical emulsification processes, surfactants play two roles: first, they reduce the interfacial tension, facilitating droplet deformation and rupture and second, they reduce droplet coalescence. Here we use a microfluidic emulsification system to completely uncouple these two processes, allowing stabilization against coalescence to be studied quantitatively, and independently of droplet formation. We demonstrate that, in addition to the classical effect of stabilization by an increase of surfactant concentration, the dynamics of adsorption of surfactant at the water-oil interface is a key element for droplet stabilization. Microfluidic emulsification devices can therefore be tailored to improve emulsification while decreasing the concentration of surfactant by increasing the time before the droplets first come into contact.

1 Introduction

Two fundamental processes occur during emulsification: droplet rupture and droplet re-coalescence. The mean droplet size of a kinetically stabilised emulsion system is governed by the relative rates of these two processes [1, 2]. Surfactants effect both processes: they reduce the interfacial tension, thereby promoting droplet rupture, and they provide a barrier to re-coalescence via the repulsive interaction between the adsorbed layers on the two colliding drops [2]. However, as droplet rupture and re-coalescence generally occur concurrently during classical emulsification processes, it has proven difficult to study the influence of the surfactant on the two processes independently

and the analysis is restricted to averaged parameters measured on large number of droplets, such as droplet sizes in bulk emulsions [1, 3]. It has, in particular, proven very difficult to study the effect of the dynamics of absorption of surfactant at the water-oil interface on emulsification. Between the formation of a new droplet and its subsequent encounter with surrounding droplets, surfactants adsorb onto the newly created interface, inhibiting re-coalescence. If the timescale of the surfactant adsorption is longer than the timescale of the collision, the fresh interface will not be sufficiently covered, leading to re-coalescence and increasing the equilibrium droplet size (EDS). This is of great industrial importance: it leads, for example, to the phenomenon of ‘over-processing’, often observed using high-pressure emulsification, in which although the energy input during emulsification has been increased, the obtained emulsions have a bigger EDS than expected [1]. Lately, new methods have been developed to prepare monodisperse emulsions [4, 5, 6]. Microfluidic devices allow the preparation of highly controlled monodisperse [6, 7, 8], bidisperse [9] as well as multiple emulsions [10, 11] or foams [12]. Because droplet-based microfluidic systems [13, 14, 15] also enable a variety of other operations, all at frequencies of kHz or higher (including splitting [16], fusion [17, 18], and sorting [19, 20]) they have broadened the range of applications of emulsions into areas such as cell-based assays [21, 22] or the synthesis of materials [23]. Microfluidic systems are also an extremely useful tool to perform fundamental quantitative studies of emulsification and emulsion stability, for example, to study droplet formation [24] or coalescence [25]. Here we use a microfluidic emulsification system to completely uncouple droplet formation and droplet re-coalescence by the control of droplet flows along cal-

ibrated channels. This allows the stabilization against re-coalescence to be studied quantitatively, and independently of droplet formation. We demonstrate how the stabilization of droplets is modified by kinetics aspects of surfactant diffusion to the oil/water interface and how this knowledge can be used to design improved microfluidic emulsification devices requiring lower concentrations of surfactant to create stable and highly monodisperse emulsions.

2 Materials and methods

Two types of microfluidic devices (M1 and M2, Figure 1) were prepared by standard soft-lithography techniques [26] in poly(dimethylsiloxane) (PDMS) with channel depths of $d_1 = 30\mu\text{m}$ (M1) or $d_2 = 75\mu\text{m}$ (M2). The PDMS was treated in an oxygen plasma oven (Gala Instrumente) and bound to a glass slide. A commercial surface coating agent (Aquapel, PPG Industries) subsequently dried with N_2 prior to use was used to decrease the wettability of aqueous phase on the channel walls. The microfluidic devices (M1) was designed to study the stability of emulsions generated on chip. It consisted of three parts (see Figure 1 (a)), (i) a classical flow focussing nozzle enabling the production of water droplets in a continuous oil phase [6], (ii) a thin channel of width $w = 50\ \mu\text{m}$ and variable length L in which the droplets are separated to prevent collision for a time $\tau \propto L$ and (iii) a coalescence chamber made of an abrupt expansion of the channel ($W = 250\ \mu\text{m}$) in which droplets randomly collide and potentially coalesce. The aqueous phase was a buffered solution (10 mM Tris-HCl, pH8.0), the oil phase a commercial fluorinated

oil (FC40, 3M, density $\rho = 1.9 \cdot 10^3 \text{ kg/m}^3$) which (i) does not cause PDMS swelling and (ii) does not solubilise most non-fluorinated organic molecules and thereby hinders the exchange of molecules between droplets through phase partitioning. An amphiphilic molecule with a fluorinated tail of a commercial oil (krytox FSH) and a hydrophilic head (di-morpholino-phosphate (DMP)) was used as a surfactant, solubilized in the oil at a concentration C (w/w) [21, 27]. The molar mass of the surfactant molecule is $M = 6.9 \cdot 10^3 \text{ g/mol}$. The critical micellar concentration (CMC) in FC40 measured by static light scattering was $C_{CMC} = 6 \cdot 10^{-5} \text{ g/g}$ ($17 \mu\text{M}$). Above the CMC , the typical radius of the micelles is $\sim 50 - 100 \text{ nm}$ ¹. Similar surfactants have proven useful for droplet-based microfluidic applications [28]. Volumetric flow rates were controlled using syringe pumps (PHD2000, Harvard Apparatus) and fixed throughout all the experiments in each of the inlet channels to $Q_o = 250 \mu\text{L/hr}$. Images of droplets in the microchannels were taken using a standard CCD camera (Guppy, Allied Vision) at 7.5 frames per seconds in region (C). The droplet size distribution was extracted by image processing (Matlab script) of ~ 1000 frames (~ 20000 droplets) by counting the number of pixels surrounded by a black ring. The number of pixels was then transformed into the surface area A of the droplet (the apparent radius R of the droplets is simply $A = \pi R^2$). For channel depth $d = 30 \mu\text{m}$, droplets of apparent radii larger than $\sim 25 \mu\text{m}$ are squeezed in the channels as flat pancakes: the droplet area A is therefore proportional to the volume in a good approximation via the approximation of the droplet shape by a cylinder.

¹A detailed description of this biocompatible surfactant as well as synthesis and characterization will be published elsewhere (Kleinschmidt et al., unpublished)

der of height d and radius R ($V = Ad$). For all the devices used, the droplet radius before coalescence was $R_0 = 24 \mu\text{m} \pm 5\%$ (for a corresponding area $A_0 = 1800 \mu\text{m}^2 \pm 10\%$). For a channel depth $d = 30 \mu\text{m}$ this corresponds to droplets of volume $V_d \sim 50 \text{ pL}$. The microfluidic device (M2) was designed to measure the build-up of surfactant molecules at the oil/water interface. It is made of a flow focussing junction and an incubation line of $100 \mu\text{m}$ width (Figure 2b). This device is interfaced with an optical setup to measure droplet fluorescence in an epifluorescence geometry. In this device, the aqueous phase was doped with resorufin at micromolar concentration in PBS buffer solution. Resorufin is used as a fluorescent marker to detect droplets, and acts as a reference for fluorescence intensity. The continuous oil phase is FC40 containing a surfactant made of the same krytox FSH tail, on which a fluorescein isothiocyanate linked to an amine terminated polyethylene oxide hydrophilic head group has been added. The synthesis of this krytox-PEO-Fluorescein surfactant will be presented elsewhere (F. Kleinschmidt et al. unpublished). This surfactant is fluorescent only when the head group is in an aqueous solution which enables the build-up at the water/oil interface to be monitored directly by the readout of droplet interface fluorescence. The fluorescence was measured by exciting the droplet with a single blue laser line (488 nm), oriented perpendicular to the microfluidic channel (See Supplementary Material). It excites both the fluorescein, bound to the surfactant, and the resorufin droplet marker: fluorescence intensities of each of the fluorophores are detected on two distinct PMTs (at 500 - 520 nm for fluorescein and at 600 - 675 nm for resorufin). We used flow rates $Q'_o = Q'_w = 200 \mu\text{L/h}$ for the oil and aqueous phases. The total flow rate in the chan-

nel after the flow focussing junction is therefore $600 \mu\text{L}/\text{hr}$, corresponding to a fluid velocity $v = 22.2 \text{ mm}/\text{s}$. This resulted in droplets of about $200 \mu\text{m}$ length. Since the width of laser line estimated from a direct microscope image is about $\sim 10 \mu\text{m}$, these elongated droplets enable the measurement of the fluorescence interface at the front of droplet to be separated from the measurement at the back of the droplet. The fluorescein signal shape was determined at four different positions along the channel, starting directly after the droplet creation point and at 2.5, 5, 7.5 and 10 mm from the nozzle. It was necessary to adjust the focal plane for each measuring position due to slight deviations from the horizontal of the microfluidic device. After changing the focal plane, the resorufin fluorescence signal was maximised at each measuring position in order to minimize noise. For the analysis, the intensity of the fluorescein signal was scaled by the resorufin signal in order to compensate the intensity variations that arise from the different focal planes. In order to reduce the noise due to the absolute signal intensity an average over 2 consecutive droplets was taken.

3 Experimental Results

First, we tested the influence of surfactant concentration on the emulsion stability using the microfluidic device M1 (Figure 1 (a)). It is clear that increasing surfactant concentrations lead to an increase of droplet stability. Fixing the length $L = 1 \text{ mm}$, we analyzed the distribution of droplet sizes in region (C) varying the concentration of the surfactant. At very low surfactant concentration – although still larger than the CMC – ($C_{CMC} \ll C < 10^{-3}$

g/g) the droplets are completely unstable: each contact between two droplets leads to coalescence [29]. At intermediate concentrations (10^{-3} g/g $< C < 2 \times 10^{-3}$ g/g, Figure 2 (a)), the droplet size distribution displays several harmonic sub-populations, at multiple integers ($i = 2, 3, \dots$) of a fundamental population ($i = 1$): fused droplets have volumes (and here areas) equal to multiple integers of the droplet volume before coalescence: each population is the consequence of a series of individual coalescence events between droplets. These droplets in region (C) are further destabilized downstream as a result of the increase of the number of collisions resulting in unstable emulsions. Finally at higher concentrations ($C > 2 \times 10^{-3}$ g/g, Figure 2(b)) the harmonic intensities decrease and become of the order of statistical noise. These stable droplets in region (C) lead to stable monodispersed emulsions that can be reliably collected and further reinjected in another microfluidic device after long-term storage in syringes (data not shown, see also [21]). Recently the deterministic nature of coalescence has been demonstrated [25]. In our case the relative proportion of each harmonic is the result of a probability of destabilization of the interface between two droplets, the stochastic nature of the process coming from the chaotic nature of the multiphase flow. In the following we will assume that this stochastic phenomenon is the same in all experiments, which is a fair assumption since all experiments are made in devices of identical dimensions and under the same flow rate conditions. The parameter $p(1)$ used to evaluate droplet stability is the proportion of unfused droplets $n(1)$ over the total number of droplets: $p(1) = n(1)/\sum in(i)$. From a practical view point, droplets are considered as stable for $p(1) > 0.999$. As expected, increasing surfactant concentration helps to stabilize droplets: at

$C = 8 \cdot 10^{-3}$ g/g, no coalescence event were observed for a total of $2.4 \cdot 10^4$ drops.

Second, we varied the length of region (B) in order to study the influence of kinetic effects on emulsion stabilization. The length of the channel in part (B) was set to values between $L = 100 \mu\text{m}$ to $L = 5 \text{ mm}$ and the droplet-size distribution was extracted for various surfactant concentrations. Since all the experiments were performed at constant total flow rate $Q = 3Q_0$ and device depth and width d and w , the length L corresponds to an ‘incubation’ time $\tau = L \times wd/Q$ during which the surfactant molecules have time to build-up at the oil/water interface. Fixing the surfactant concentration to $C = 10^{-3}$ g/g, an increase of the length L lead to a decrease of the number of coalescence event (see Figure 3). The experiment was repeated over a wide range of length and surfactant concentrations (see Figure 4). An increase of L led to a smaller proportion of coalesced droplets (Figure 4), $p(1)$ increased when L increased. In order to quantify the transition, $p(1)$ was plotted as a function of the parameter LC^2 for all the experimental data collected (Fig. 4, the origin of this scaling law will be explained later in this article). We observed a clear transition between the regime of stable droplets and unstable droplets (Fig. 4): experimentaly the separation between the two regimes is in a good approximation represented by Eq. 1:

$$LC^2 = k \tag{1}$$

where $k \sim 10^{-9} \text{ m}(\text{g/g})^2$ depends on the surfactant used: for other surfactant we observed similar transition but at different values (data not shown).

For values of $LC^2 \gg 10^{-9} \text{ m(g/g)}^2$ the droplets are stable while for values of $LC^2 \ll 10^{-9} \text{ m(g/g)}^2$ the droplets are unstable. This sharp transition showed that two parameters are relevant for the stabilization of a droplet interface: the surfactant concentration in the oil phase and an additional time-scale corresponding to the droplet incubation time with the surfactant molecules.

In order to demonstrate that this time-scale is linked to the kinetics of build-up of the interface we have used the microfluidic device (M2) with the fluorescent surfactant and interfaced the microfluidic chip with the laser-induced fluorescence set-up. Although less efficient for droplet stabilization, it enabled stable droplets to be produced at 0.05 g/g and displayed the same type of behaviour, i.e. an increased stability of the emulsion with LC^2 (data not shown). The surfactant has been designed in such a way that the fluorescence is quenched when the hydrophilic head group is in the oil phase and fluorescent when in water. Therefore the fluorescence of the molecules is linked to the presence of the surfactant at the oil/water interface. For this experiment we produced large elongated droplets at a microfluidic junction with larger dimensions (see materials and methods). The increase of droplet size increased the fluorescent signals coming solely from the molecules at the interface. The profiles of the fluorescein signal along the droplets are presented in Figure 5 for various measurement points along the incubation channel corresponding to different ages of the droplets since their formation. Directly after the creation the fluorescence profiles of the droplet are very asymmetric: virtually no fluorescent signal is measured in the middle and front end of the droplet and the maximum of intensity is at the back of the

droplet (Figure 5). Upon following the droplet down the channel the signal gradually rises from the back end towards the middle and finally the front end of the droplet. At the end of the channel (10 mm) the profile is still asymmetric with an excess of surfactant at the back end of the droplet. This asymmetry has also been observed for other flow rates (data not shown). The build-up of the interface is therefore a function of time: the incubation of the droplet along the channel leaves time to the surfactant to adsorb at the oil/water interface. In addition these data show that the surfactant does not accumulate symmetrically on the surface of the droplets. Instead the back end (Figure 5) of the droplet is already highly charged with surfactant at the first measurement position directly after the creation of the droplet. The droplet interface then gradually fills up with surfactant molecules from the back end towards the middle and finally the front end. This feature of interface in presence of surfactant molecules in a flow or in an electric field can ultimately lead to tip-streaming [30]. These data confirm that the build-up of surfactant at the interface occurs in microfluidic channels on a time-scale of the order of the typical time-scale of droplet manipulation (ms - s). It is clear that this build-up of surfactant at the interface and the kinetics of the surfactant adsorption becomes the key parameters controlling emulsion stability, and are more important than thermodynamic equilibrium parameters such as surface tension or *CMC* values.

4 Discussions

In the following we will discuss our experimental observations to explain the behaviour observed in these very simple microfluidic devices. Our aim is to focus on the build-up of the interface as an average over the whole droplet profile, i.e. neglecting the description and modeling of the asymmetric profile observed here. Indeed such an approach would require the description of the motion of molecules at a complex interface in the presence of two flow patterns which is way beyond the scope of the present manuscript. Based on the experimental observations of the dynamic effect of interface build-up, we will discuss the influence of convection and diffusion of micelles and monomers to the droplet/oil interface between the time of droplet production to the time where droplets touch each other. Over the time-scale of droplet production ($\lesssim 10^{-3}$ s), all of the surfactant is dispersed in the oil volume and effectively none at the oil-water interface. This is confirmed by the experimental observation that the frequency of droplet production is independent of the concentration of surfactant: at short time-scales, there is no effect of surfactant on the surface tension, the droplet production frequency is controlled by the oil/water surface tension only. Over a longer time-scale surfactant molecules migrate to and build-up at the interface. At this stage both concentrations and kinetics of adsorption at the interface are important [31]. To start with, we discuss why, in our opinion, diffusion dominates the kinetics of stabilization by the surfactant. Usually, in order to estimate whether diffusive or convective transport is dominating in a system, the Peclet number $Pe = UL/D$ is calculated, with U , L and D as the typical velocity, length-

scale and diffusion coefficient in the system. In our case, the Peclet number calculated with a droplet size of $50\ \mu\text{m}$, a typical speed of $0.1\ \text{m/s}$ and diffusion coefficient of $10^{-10}\ \text{m}^2/\text{s}$ ($Pe = 5000$) is larger than one which indicates the predominance of convection.

However in our case, in the reference frame of the droplet, the oil between two droplets is rotating with a laminar flow pattern (Fig. 6) [32, 33, 34]. The flux towards the droplet is then balanced by the flux outwards: the effective transport of elements by convection is not directly linked to the speed of the droplets. However, it could be argued that a certain degree of asymmetry in the oil flow profile could lead to a net flux towards the droplet. Such an asymmetry is for example a known feature for the so-called Taylor bubble which displays stagnation points of the continuous phase streamlines at the edge of bubbles rising in capillaries in a steady continuous phase [33]. In our case, the continuous oil phase moves at the same speed as the droplet which pushes the stagnation point to the edge of the droplet [32]. Therefore, this asymmetry would be small but could promote the adsorption of surfactant molecules at the back of the droplet which then could explain the asymmetric fluorescent profile obtained in Figure 5. The most effective source of molecule transport in our case will then be diffusive effects: they enable transport of surfactant towards the interface across the laminar flow lines.

During the flow of the droplet in the channel, the interface adsorbs a certain number of surfactant molecules from the bulk phase. Geometrically, the maximum packing of molecules of typical lateral dimension $\delta \sim 2\ \text{nm}$ at the interface of a droplet of radius R is achieved with n molecules when

$4\pi R^2 = n\delta^2$. Droplets will be stable when the number of molecules at the interface is larger than a fraction $0 < f < 1$ of the maximum packing, therefore the stability condition reads:

$$n \gtrsim 4f\pi R^2/\delta^2 \quad (2)$$

As discussed previously, only diffusive effects are considered to describe the build-up of the interface. In the oil, two species are present: free surfactant molecules at a concentration equal to the *CMC* and micelles which represent the majority of the surfactant concentration C . Considering the sizes of the micelles (~ 75 nm) the diffusion coefficient D_{free} of the free surfactant molecules is much larger than the diffusion coefficient of the micelles D_{mic} and is therefore expected to dominate the diffusion process. The n free surfactant molecules required to stabilize the droplet interface are dispersed in a volume surrounding the droplet over a distance ε of the droplet interface: $n \sim 4\pi R^2 \varepsilon C_{CMC} N_A$ where $N_A = 6.10^{23}$ mol⁻¹ is Avogadro's number. In a diffusion-limited process, the molecules in this volume will reach the interface in a time $t_{free} \sim \varepsilon^2/D_{free}$ which is therefore expressed as Eq. 3:

$$t_{free} \sim \frac{f^2}{N_A^2 C_{CMC}^2 \delta^4 D_{free}} \quad (3)$$

Eq. 3 can be further derived to determine the stability transition. Indeed since $t = Lwd/Q$ the stability condition now reads:

$$L \sim \frac{f^2}{\delta^4 C_{CMC}^2 D N_A^2} \times \frac{Q}{wd} \quad (4)$$

The fact that the stability condition does not depend on surfactant concentration is contradictory to the experimental observations (Figure 4). Diffusion of free-surfactant molecules is therefore not the main mechanism of the build up of the interface leading to droplet stabilization. Micelle diffusion has therefore to be considered. Micelles of radius $r = 75$ nm diffuse much more slowly than free surfactant molecules but when a micelle reaches the interface, the number of molecules involved is given by the number of monomers in a micelle ($\sim 4r^2/\delta^2 \gg 1$). Now the n surfactant molecules are present in a smaller volume surrounding the droplet: $n \sim 4\pi R^2 \varepsilon C N_A$ and they will pack the interface in a time t_{mic} , the time required for a sufficiently large number of micelles to diffuse to the interface:

$$t_{mic} \sim \frac{f^2}{N_A^2 C^2 \delta^4 D_{mic}} \quad (5)$$

Eq. 5 can be further derived to determine the stability transition:

$$LC^2 \sim \frac{f^2}{\delta^4 D N_A^2} \times \frac{Q}{wd} \quad (6)$$

Eq. 6 correctly reproduces that the relevant parameter for droplet stabilization is LC^2 . In addition, when combining the experimental values $D_{mic} = 10^{-12}$ m²/s, $Q = 750$ μ L/hr, $w = 50$ μ m and $d = 30$ μ m, and the experimental value of the transition ($k \sim 10^{-9}$ m(g/g)²) we find $f \sim 0.1$: the interface is stabilized by a fraction of about 10 % of the maximum packing that can be obtained with 2 nm molecules at the surface of the droplet. This corresponds to a time-scale $t_{mic} \sim 1 - 50$ ms depending on the surfactant concentration.

This timescale corresponds to the one observed in the experiments: a droplet needs ~ 35 ms to travel a 5 mm long channel of 50 μm width and 30 μm depth. Therefore, the experimental observations are consistent with a model of the interface build-up based on a diffusion limited process involving surfactant micelles. The model enables the fraction of molecules at the interface required to stabilize the emulsion to be extracted from the experimental data.

The dynamics of the stabilization is reasonably explained by simple arguments involving micellar diffusion and the analysis performed here enables an estimation of the density of molecules at the interface required to stabilize an emulsion. These results not only show the importance of the kinetics of surfactant adsorption at the interface on stabilization of an emulsion but they also demonstrate that microfluidic systems are an efficient tools to obtain fundamental information on the physical-chemistry of a surfactant molecule. We are currently using this technique as a way to characterize surfactants for biological applications (Kleinschmidt et al., in preparation) and we believe that this type of analysis will be of great value to the final users of droplet-based technology.

Practically, microfluidic emulsification has a very interesting advantage. Contrary to bulk emulsification – in which droplet collisions are coupled to droplet production [3] – droplet production and droplet collisions can be decoupled by the use of an ‘incubation’ channel which enables the surfactant concentration required to stabilize the emulsion to be decreased. The number of micelles in solution after emulsification can be decreased by the use of an ‘incubation’ nozzle. Since transport phenomena (Ostwald ripening, solubilisation

exchange) in emulsions [2] are mediated by micellar transport, the emulsion produced will be less sensitive to these transport phenomena.

5 Conclusions

In summary, we have observed and quantified the influence of surfactant kinetics on the stabilization of droplets in two-phase flow microfluidics, using two different approaches, one based on a coalescence study and the other based on fluorescence measurement of surfactant build-up at the oil/water interface. The build-up of the molecules at the interface is measured by the increase of the fluorescence signal at the interface and shows an asymmetric profile between the rear and the front of the droplet. The dynamic build-up of the interface is linked to the stabilization of the emulsion produced on-chip: by incubating droplets in a channel where they do not touch, the surfactant is given enough time to pack at the interface leading to the stabilization of droplets with lower surfactant concentration. This dynamic process is mainly governed by diffusion of the surfactant micelles. From our simple experiments we have been able to extract a value for the density of molecules at the interface required to stabilize droplets against coalescence. Finally, we believe that these results and methods will help the design of microfluidic devices for a better control of emulsion properties and for the characterization of surfactant in order to obtain information on typical behaviour of molecules at an interface on a millisecond timescale.

6 Acknowledgements

The authors thank B. Hutchison (Raindance Technologies - USA), D. A. Weitz (Harvard University - USA), J. Bibette (ESPCI - F) and C. Baroud (LadHyX - F) for stimulating and interesting discussions. J.-C. B. was supported by an EMBO long-term fellowship [ALTF 915-2006]. This work was supported by the European Network MiFem under Contract No. 028417, the Ministre de l'Enseignement Suprieur et de la Recherche, Centre National de la Recherche Scientifique (CNRS), Agence National de la Recherche (ANR) (ANR-05-BLAN-0397), and the Fondation d'entreprise EADS.

7 Supporting Information Available

Sketch of the optical set-up for on-chip fluorescence measurement. This material is available free of charge via the Internet at <http://pubs.acs.org>.

References

- [1] S. M. Jafari, E. Assadpoor, Y. He, and B. Bhandari. *Food Hydrocolloids* **2008**, 22, 1191–1202.
- [2] J. Bibette, F. Leal-Calderon, and P. Poulin. *Rep. Prog. Phys.* **1999**, 62, 696–1033.
- [3] L. Lobo and A. Svereika. *J. Colloid Interface Sci* **2003**, 261, 498–507.
- [4] P. B. Umbanhowar, V. Prasad, and D. A. Weitz *Langmuir* **2000**, 16, 347–341.

- [5] T. Thorsen, R. W. Roberts, F. H. Arnold, and S. R. Quake. *Phys. Rev. Lett.* **2001**, 86, 4163–4166.
- [6] S. L. Anna, N. Bontoux, and H. A. Stone. *Appl. Phys. Lett.* **2003**, 82, 364–366.
- [7] C. Priest, S. Herminghaus, and R. Seemann. *Appl. Phys. Lett.* **2006**, 88, 024106.
- [8] G. F. Christopher and S. L. Anna. *Journal of Physics D: Applied Physics* **2007** 40, R319–R336.
- [9] L. Frenz, J. Blouwolf, A. D. Griffiths, and J.-C. Baret. *Langmuir* **2008**, 24, 12073–12076.
- [10] L.-Y. Chu, A. S. Utada, R. K. Shah, J.-W. Kim, and D. A. Weitz. *Angew. Chem. Int. Ed.* **2007**, 46, 8970–8974.
- [11] N. Pannacci, H. Bruus, D. Bartolo, I. Etchart, T. Lockhart, Y. Hennequin, H. Willaime, and P. Tabeling. *Phys. Rev. Lett.* **2008**, 101, 189901.
- [12] D. Weaire and W. Drenckhan. *Adv. Colloid Interface Sci* **2008**, 137, 20–26.
- [13] T. M. Squires and S. R. Quake. *Rev. Mod. Phys.* **2005**, 77, 977–1026, 2005.
- [14] G.M. Whitesides, D. Janasek, J. Franzke, A. Manz, D. Psaltis, S. R. Quake, C. Yang, H. Craighead, A.J. deMello, J. El-Ali, P.K. Sorger,

- K.F Jensen, P. Yager, T. Edwards, E. Fu, K. Helton, K. Nelson, M.R. Tam, and B.H. Weighl. *Nature* **2006**, 442, 367–418.
- [15] B. T. Kelly, J.-C. Baret, V. Taly, and A. D. Griffiths. *Chem. Commun.* **2007**, 18, 1773–1788.
- [16] D. R. Link, S. L. Anna, D. A. Weitz, and H. A. Stone. *Phys. Rev. Lett.* **2004**, 92, 054503.
- [17] K. Ahn, J. Agresti, H. Chong, M. Marquez, and D. A. Weitz. *Appl. Phys. Lett.* **2006** 88, 264105.
- [18] C. Priest, S. Herminghaus, and R. Seemann. *Appl. Phys. Lett.* **2006** 89, 134101.
- [19] K. Ahn, C. Kerbage, T. P. Hunt, R. M. Westervelt, D. R. Link, and D. A. Weitz. *Appl. Phys. Lett.* **2006** 88, 024104.
- [20] L. M. Fidalgo, G. Whyte, D. Bratton, C. F. Kaminski, C. Abell, and W. T. S. Huck. *Angew. Chemie Int. Ed.* **2008**, 47, 2042–2045.
- [21] J. Clausell-Tormos, D. Lieber, J.-C. Baret, A. El-Harrak, O. J. Miller, L. Frenz, J. Blouwolf, K. J. Humphry, S. Kster, H. Duan, C. Holtze, D. A. Weitz, A. D. Griffiths, and C. A. Merten. *Chem. Biol.* **2008**, 15, 427–437.
- [22] S. Koester, F. E. Angil, H. Duan, J. J. Agresti, A. Wintner, C. Schmitz, A. C. Rowat, C. A. Merten, D. Pisignano, A. D. Griffiths, and D. A. Weitz. *Lab-on-a-Chip*, **2008**, 8, 1110–1115.

- [23] L Frenz, A. El-Harrak, M. Pauly, S. Begin-Colin, A.D. Griffiths, and J.-C. Baret. *Angew. Chemie Int Ed.* **2008**, 47, 6817–6820.
- [24] S. L. Anna and H. C. Mayer. *Phys. Fluids* **2006**, 18, 121512.
- [25] N. Bremond, A. R. Thiam, and J. Bibette. *Phys. Rev. Lett.* **2008**, 1, 024501.
- [26] Y. N. Xia and G. M. Whitesides. *Annu. Rev. Mater. Sci.* **1998**, 28, 153–184.
- [27] WO/2008/021123A1. Fluorocarbon emulsion stabilizing surfactants, 2008.
- [28] C. Holtze, A. C. Rowat, J. J. Agresti, J. B. Hutchison, F. E. Angil, C. H. J. Schmitz, S. Kster, H. Duan, K. J. Humphry, R. A. Scanga, J. S. Johnson, D. Pisignano, and D. A. Weitz. *Lab-on-a-Chip* **2008**, 8, 1632–1639.
- [29] Y. C. Tan, Y. L. Ho, and A. P. Lee. *Microfluidics and Nanofluidics* **2007**, 3, 495–499.
- [30] C. D. Eggleton, T.-M. Tsai, and K. J. Stebe. *Phys. Rev. Lett.* **2001**, 87, 048302.
- [31] B. V. Zhmud, F. Tiberg, and J. Kizling. *Langmuir* **200**, 16, 2557–2565.
- [32] A. Guenther, M. Jhunjhunwala, M. Thalmann, M. A Schmidt, and K. F. Jensen. *Langmuir* **2005**, 21, 1547–1555.
- [33] A. Guenther and K. F. Jensen. *Lab-on-a-Chip* **2006**, 6, 1487–1503.

- [34] P. Garstecki, M. J. Fuerstman, H. A. Stone, and G. M. Whitesides.
Lab-on-a-Chip **2006**, 6, 437–446.

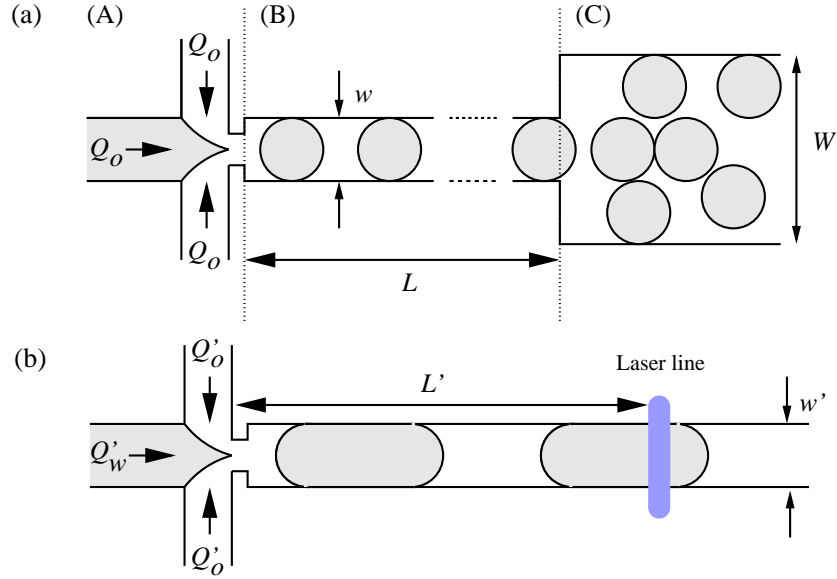


Figure 1: Diagram of the microfluidic devices (M1) and (M2) for surfactant analysis. (a) M1 used for coalescence studies: the device of depth $30 \mu\text{m}$ consists of three different part: (A) a hydrodynamic flow focussing junction, (B) a channel to keep droplets separated for a length L ($w = 50 \mu\text{m}$), (C) a coalescence chamber where the droplet undergo stochastic collision for the test of emulsion stability ($W = 250 \mu\text{m}$). The flow rates are fixed at $Q_o = 250 \mu\text{L/hr}$. (b) M2 used for the analysis of surfactant build-up at the interface (the depth of the channel is $75 \mu\text{m}$). The droplet production junction is coupled to an optical setup for fluorescence analysis in the incubation channel ($w' = 100 \mu\text{m}$). The flow rates are $Q'_o = 200 \mu\text{L/hr}$ and $Q'_w = 200 \mu\text{L/hr}$ in order to produce elongated droplets, of length larger than the width of the laser line (in blue).

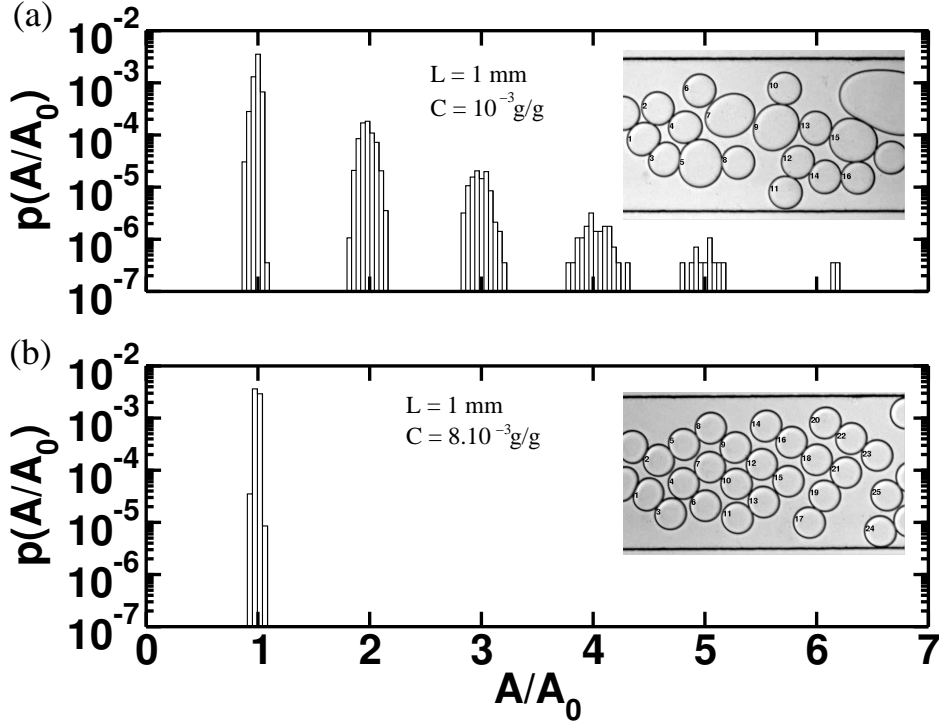


Figure 2: Droplet stability as a function of surfactant concentration C : size distribution of droplets in the coalescence chamber. The length L of the nozzle is $L = 1 \text{ mm}$ ($\tau = 7.2 \text{ ms}$) for two surfactant concentrations. The area of droplets A are rescaled by the area of unfused droplet A_0 . (a) $C = 10^{-3} \text{ g/g}$, the emulsion is unstable ($A_0 = 1914 \mu\text{m}^2$), several populations are visible, at areas equal to multiple integers of the unfused droplet area, (b) $C = 8 \cdot 10^{-3} \text{ g/g}$, the proportion of fused droplets is less than 10^{-4} ($A_0 = 1734 \mu\text{m}^2$): increasing surfactant concentration increases the emulsion stability. For the measurement, droplets touching the edges of the image are discarded.

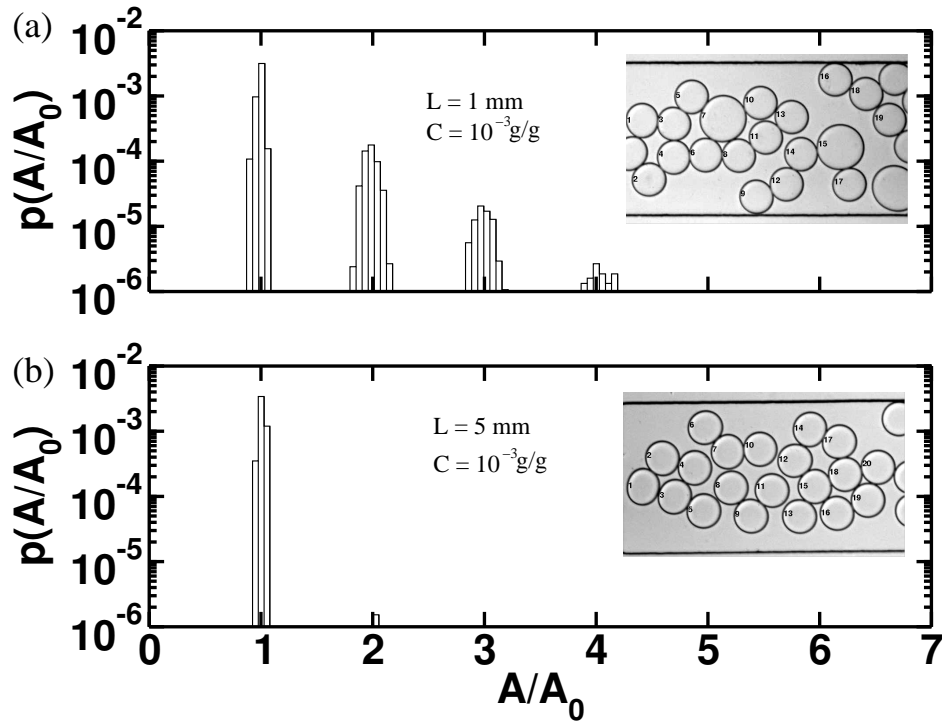


Figure 3: Droplet stability as a function of incubation length L : size distribution of droplets in the coalescence chamber. The concentration $C = 10^{-3} \text{ g/g}$ is constant. (a) $L = 1 \text{ mm}$ ($\tau = 7 \text{ ms}$), the emulsion is unstable ($A_0 = 1914 \mu\text{m}^2$), (b) $L = 5 \text{ mm}$ ($\tau = 36 \text{ ms}$), the proportion of fused droplets is less than 10^{-3} ($A_0 = 2028 \mu\text{m}^2$): increasing the length of the channel after production helps stabilizing emulsions.

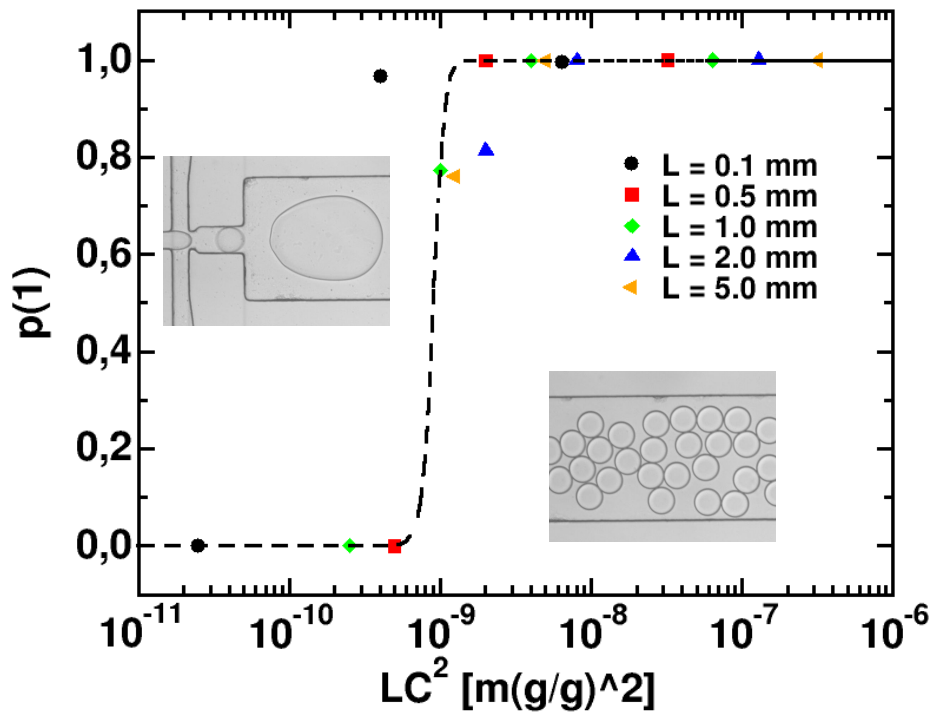


Figure 4: Droplet stability analysis. The ratio of non fused droplets is plotted for five lengths L and various surfactant concentrations C . Both an increase of length and surfactant concentration help to stabilize the droplets: the coalescence rate displays a sharp transition as a function of LC^2 .

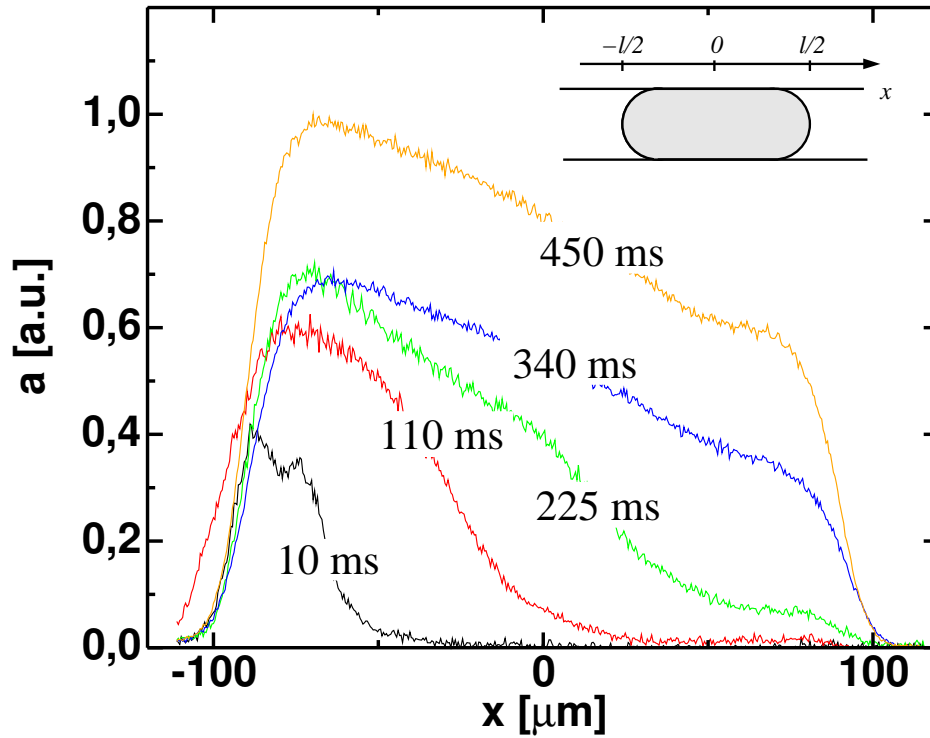


Figure 5: Fluorescent signal intensity a in arbitrary units of the surfactant as function of the position of the laser line along the droplet x . Fluorescent intensity profiles are given for different position along the channel (0, 2.5, 5, 7.5 and 10 mm). The label of each curve corresponds to the droplet lifetime (in ms) after generation when they pass the laser line. Each presented curve is an average over 2 droplets to reduce noise due to low absolute signal intensity. The surfactant builds up at the water/oil interface from the back of the drop to the front.

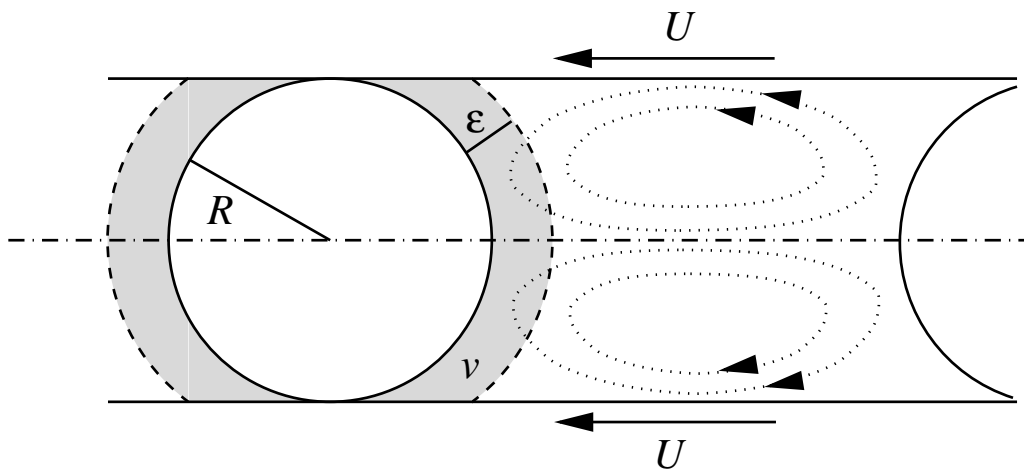


Figure 6: Sketch of the droplet in the microchannel. In the frame of the droplet, the rotating motion of the oil results in an almost zero net flux of the surfactant towards the droplet interface [32, 33]. In the vicinity of the droplet, diffusion enables micelles to reach the droplet interface. The number of surfactant molecules in the volume v surrounding the droplet is sufficient to stabilize the interface by simple diffusion of the micelles over the distance ε .

8 For table of contents use only

Kinetic aspects of emulsion stabilization by surfactants : a microfluidic analysis

Jean-Christophe Baret, Felix Kleinschmidt, Abdeslam El Harrak, and Andrew D. Griffiths

